

Toward a simple topological model of a three-phase transformer including deep saturation conditions

Model of a three-phase transformer

1161

Sergey E. Zirka

Department of Physics and Technology, Dnipro National University, Dnipro, Ukraine

Dennis Albert

Institute of Electrical Power Systems, Graz University of Technology, Graz, Austria

Yuriy I. Moroz

Department of Physics and Technology, Dnipro National University, Dnipro, Ukraine

Lukas Daniel Domenig

Institute of Fundamentals and Theory of Electrical Engineering, Graz University of Technology, Graz, Austria, and

Robert Schürhuber

Institute of Electrical Power Systems, Technische Universität Graz, Graz, Austria

Received 19 December 2022
Revised 30 July 2023
Accepted 18 August 2023

Abstract

Purpose – This paper aims to propose a method of parametrizing topological transformer model at high flux densities in the core.

Design/methodology/approach – The approach proposed is based on terminal voltages and currents measured in a special purpose saturation test whose data are combined with typical saturation curves of grain-oriented electrical steels; the modeling is carried out in the ATPDraw program.

Findings – The authors corroborate experimentally the necessity of dividing the zero sequence impedance between all transformer phases and propose a method of the individual representation of the legs and yokes. This eliminates the use of nonexistent leakage inductances of primary and secondary windings.

Practical implications – The presented modeling approach can be used for predicting inrush current events and in the evaluation of the impact caused by geomagnetically induced currents (GICs).



© Sergey E. Zirka, Dennis Albert, Yuriy I. Moroz, Lukas Daniel Domenig and Robert Schürhuber. Published by Emerald Publishing Limited. This article is published under the Creative Commons Attribution (CC BY 4.0) licence. Anyone may reproduce, distribute, translate and create derivative works of this article (for both commercial and non-commercial purposes), subject to full attribution to the original publication and authors. The full terms of this licence may be seen at <http://creativecommons.org/licences/by/4.0/legalcode>

COMPEL - The international journal for computation and mathematics in electrical and electronic engineering
Vol. 42 No. 5, 2023
pp. 1161-1172
Emerald Publishing Limited
0332-1649
DOI 10.1108/COMPEL-12-2022-0427

Originality/value – The proposed approach is completely original and will contribute to a better understanding of the transients occurring in a transformer under abnormal conditions, such as inrush current events and GICs.

Keywords Transformer model, Core saturation, Zero sequence representation

Paper type Research paper

1. Introduction

The ever-growing number of publications on transformer modeling under saturation conditions, for instance, during inrush current events and geomagnetically induced currents (GICs), shows that this problem remains far from being solved. Among the reasons for the appearance of new papers is that any transformer model shows certain inrush currents. This creates the illusion about the easiness of creating an appropriate transformer model and often leads to hasty conclusions. It is not seldom when some developers uncritically adopt well-known transformer models, which obviously do not reflect the physics of the phenomena in transformers with saturated magnetic system. Typical errors here are the use of individual (nonexistent) leakage inductances of individual windings and merging legs and yokes into indivisible core branches (Fuchs and You, 2002; Pedra *et al.*, 2004; Moses *et al.*, 2010). The latter implies the concentration of transformer zero sequence (ZS) impedance at the center leg, which always leads to overestimated inrush currents, as will be shown below.

It would seem that simulation errors should be detected experimentally, but unfortunately, experiments related to inrush currents are not always trustworthy. This is due to the influence of the residual core fluxes, the ohmic resistance of the excited winding (especially in small and scaled-down transformers) and neglected parameters of the supply network.

The objective of this paper is to extend the discussion of these issues in Zirka *et al.* (2022), where a full-scale saturation test (Albert *et al.*, 2021) on a three-phase 50 kVA transformer was simulated using a catalog-based dynamic hysteresis model (DHM). The concept of the composite DHM was proposed in (Zirka *et al.*, 2014), while implementation details of the model are documented in (Zirka *et al.*, 2015a) and (Zirka *et al.*, 2015b) for its static and dynamic components.

Unlike the complicated modeling approach in Zirka *et al.* (2022), a direct use of the saturation test results is proposed in this paper in combination with typical saturation curves of conventional and high permeability grain-oriented electrical steels used in transformers (Figure 1), denoted as T74 and T90, respectively, according to the years of their manufacturing in 1974 and 1990.

2. Topological transformer models and their parameters

Since the models developed in this paper are intended to be used in transient network simulators, it seems appropriate to create them in the form of electrical equivalent schemes instead of using notoriously slow finite-element models (Bíró *et al.*, 2008; Chisepo *et al.*, 2018). The modeling approach developed in this study is based on the known topological models of Martínez *et al.* (2005), Chiesa *et al.* (2010) and Zirka *et al.* (2018). Although these studies describe in detail the structures of transformer models, some questions remain open regarding their parameters, especially those determining transformer behavior under saturation conditions.

To make the paper self-consistent and explain the uncertainties in model parameters, magnetic and electric models of a three-legged two-winding transformer are represented in Figure 2. Hysteretic reluctances of the legs (\mathcal{R}_A , \mathcal{R}_B and \mathcal{R}_C) and yokes (\mathcal{R}_{AB1} , \mathcal{R}_{AB2} , \mathcal{R}_{BC1}



Source: Authors' own work

Figure 1.
Tested and modeled
50 kVA transformers:
T74 (left) and T90
(right)

and \mathfrak{R}_{BC2}) are shown in the structural transformer model of Figure 2(a). In Figure 2(b), nonlinear reluctances of the upper and lower yokes are joined into reluctances \mathfrak{R}_{AB} ($= \mathfrak{R}_{AB1} + \mathfrak{R}_{AB2}$) and \mathfrak{R}_{BC} ($= \mathfrak{R}_{BC1} + \mathfrak{R}_{BC2}$). The rest of the model reluctances are elements representing magnetic flux paths in air/oil. Among them, reluctances \mathfrak{R}_{12} characterize the leakage channels between the windings, and each \mathfrak{R}_{01} represents the insulation clearance between the inner, low-voltage (LV) winding and the core leg. Three individual per-phase reluctances \mathfrak{R}_0 , which represent the ZS flux paths, separate the legs and yokes that make the model topological. When approaching saturation, an increasing part of the core flux closes through \mathfrak{R}_0 , resulting in substantially different magnetic fluxes in the legs and yokes.

In the schematic magnetic model of Figure 2(b), magneto-motive forces F_1 and F_2 (with corresponding indexes) represent the inner and outer windings, respectively. Reluctances \mathfrak{R}_G takes into account the air gaps at core joints.

A duality-derived electric transformer model is shown by elements placed between six ideal transformers (ITs) in Figure 2(c). The legs and yokes are represented here by the DHM-inductors from the ATPDraw menu (Høidalen *et al.*, 2021), which are used in this study as static hysteresis models (SHM). Resistors R_L are used to adjust the model to the measured loss. Linear inductances L of the model have the same subscripts as the linear reluctances \mathfrak{R} in the magnetic model of Figure 2(b). Their values are linked by the relationship $L = N_1^2 / \mathfrak{R}$, where N_1 is the number of turns in the inner LV winding. The 1:1 turn ratio of three IT₁ at LV terminals means that the model parameters are referred to N_1 turns. So, the turn ratio n of the IT₂ at the high voltage (HV) terminals is N_1/N_2 , where N_2 is the number of turns in the outer HV winding. Therefore, r_1 and r_2 are real (nonreferred) resistances of the LV and HV windings.

As a part of the ZS flux is closed through the tank and structural parts, associated iron losses are accounted for by resistors R_0 connected in parallel with inductances L_0 . The values of L_0 and R_0 are evaluated using active and reactive powers measured in the ZS test (Martinez *et al.*, 2005; Zirka *et al.*, 2022).

Leakage inductance L_{12} is computed from the nameplate short-circuit reactance, then inductance L_{01} can be supposed to be equal to $0.5L_{12}$ (Chiesa *et al.*, 2010) as a first approximation. Per phase capacitances C on the HV side are used to reproduce the cobra-type hysteresis loops observed in the measurements, see Figure 3.

The increase of C rotates the calculated loop anticlockwise, whereas the increase of core gaps (i.e. decreasing L_G) has the opposite effect. The model fitting can be started with arbitrarily large or absent L_G .

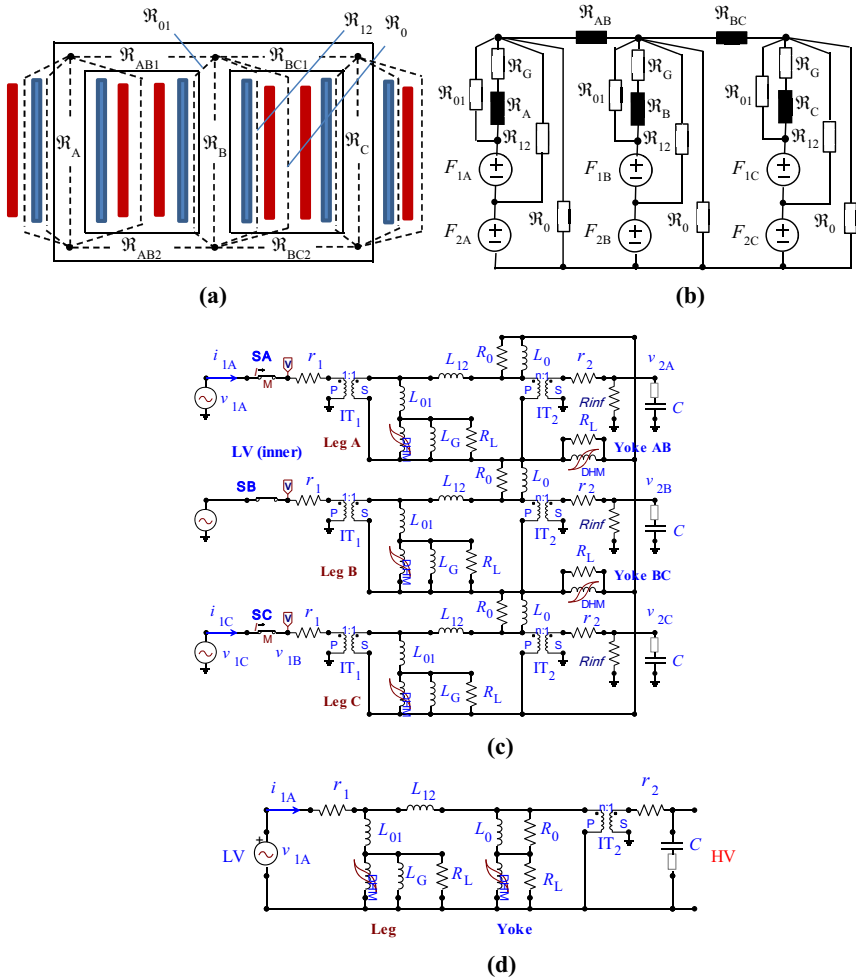


Figure 2. Transformer models: (a) physical structure; (b) magnetic model; (c) ATPDraw electric model of the unloaded YNyn0 transformer; (d) electric model of Phase A applicable to the saturation test (only)

Source: Authors' own work

3. Core parts representations

3.1 Dynamic hysteresis model-based prerequisites for simplified transformer modeling

There are no direct methods for identifying ψ - i characteristics of the legs and yokes individually. Therefore, most frequently, the outer legs and adjoining yokes are combined into indivisible "limbs" whose magnetization curves can be measured using single-phase techniques described in Fuchs and You (2002). The use of such obtained ψ - i curves implies the usage of a transformer model, which has a single ZS branch placed at the center leg. As shown in Zirka *et al.* (2022), this model becomes inaccurate as the core approaches saturation. This is because the yokes are saturated to lower levels than those achieved by deeply saturated legs. An important caveat made by Fuchs and You (2002) is that the

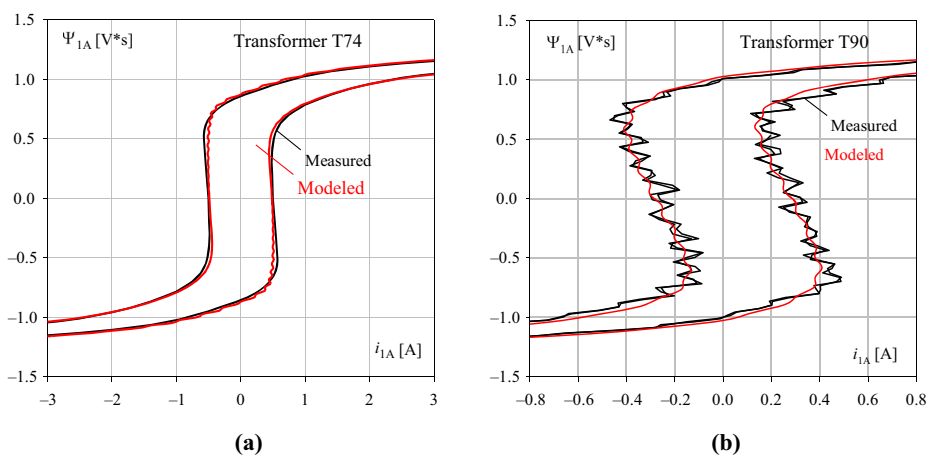


Figure 3.
Measured and
calculated terminal
loops of transformers
T74 (a) and T90 (b)

Source: Authors' own work

influence of the tank is neglected in the derivations. The latter means neglecting any ZS paths that, in turn, supposes excitation levels insufficient for deep saturation of the core.

A saturation test with substantially increased single-phase voltages was recently proposed in [Albert et al., 2021](#). Its idea is to saturate the outer legs (A and C) of the unloaded transformer by applying equal antiphase voltages (v_{1A} and v_{1C}) to the inner, LV windings of these legs. To simulate the test in the model of [Figure 2\(c\)](#), switch S_B should be open and $v_{1C}(t) = -v_{1A}(t)$. In this case, the flux in the center leg B vanishes, which makes Phases A and C of the core magnetically decoupled. This allows one to consider processes either in Phase A or Phase C. Taking for definiteness Phase A, the model in [Figure 2\(c\)](#) is reduced to the circuit in [Figure 2\(d\)](#) where IT_1 is unnecessary. As compared to Phase A of the full model in [Figure 2\(c\)](#), the model in [Figure 2\(d\)](#) produces exactly the same electric and magnetic outputs but is more convenient for explaining the novel modeling approach.

Following [Zirka et al. \(2022\)](#), the quality of the model in [Figure 2\(d\)](#) is evaluated by its ability to reproduce the terminal curves $\psi_{1A}-i_{1A}$ obtained at increased ($V_{\text{peak}} = 420$ V) and rated ($V_{\text{peak}} = 325$ V) sinusoidal voltage v_{1A} . When building loops 1 and 3 in [Figure 4](#), the value ψ_{1A} is calculated by integrating the difference ($v_{1A}-r_1 i_{1A}$), that is, the measured voltage v_{1A} minus the voltage drop across resistance r_1 .

In the absence of $\psi-i$ characteristics of the legs and yokes, the model fitting in [Zirka et al. \(2022\)](#) was made by using the DHM inductors, which use a list of predefined materials. Key components of the DHM are a SHM combined with a single-valued saturation curve, which ends at the level of technical saturation (near 2.0–2.03 T). In addition to the brief description in ([Høidalen et al., 2021](#)), it should be mentioned here that the DHM-inductor (Zirka–Moroz $L(i)$ hysteresis model) allows the users to create their own static loops and the saturation curves. This makes this element a flexible tool for reproducing $B-H$ curves of arbitrary shape. Other distinguishing features and advantages of the SHM are described in ([Zirka et al., 2014](#)).

Here, a choice should be made between conventional grain-oriented (CGO) steels and high-permeability grain-oriented (HGO) steels. [Figure 5](#) shows saturation curves of typical HGO and CGO steels extended beyond the points (1, 2 and 3) of their technical saturation. It can be seen in [Figure 5](#) that catalog saturation curves of CGO steels M4 and M5 are quite close to each other. The same situation can be observed in [Figure 4](#) of ([Hernández et al., 2011](#)), where $B-H$ curves of

CGO steels M4, M5 and M6 are merged at $B > 1.6$ T. Therefore, for definiteness and due to the year of manufacturing transformer T74 (1974), conventional grain-oriented (GO) steel M5 was chosen in Zirka *et al.* (2022) as a core material.

To reproduce the “rounded” loop 1 in Figure 4 (i.e. the loop measured at $V_{\text{peak}} = 420$ V), the concept of the variable core gap has been implemented in Zirka *et al.* (2022), where variable inductances L_G were used in the model of Figure 2(c). It was shown in Zirka *et al.* (2022) that the flux-current curve of the nonlinear inductance L_G has to be found anew for each new value of the terminal capacitances C . This complicates the fitting of the model with

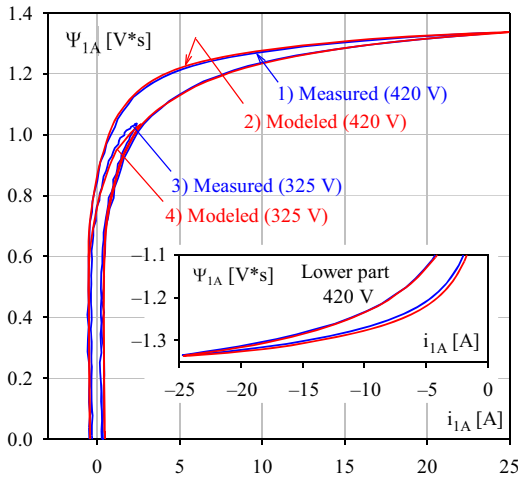


Figure 4.
Measured and modeled terminal loops of transformer T74

Source: Authors' own work

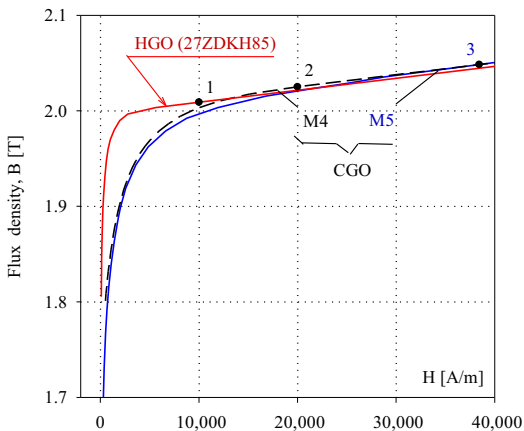


Figure 5.
Saturation curves of HGO and CGO steels

Source: Authors' own work

variable L_C and makes it advisable to base the transformer model on the measured loop $\psi_{1A}-i_{1A}$.

3.2 Transformer modeling based on the terminal loop $\psi_{1A}-i_{1A}$

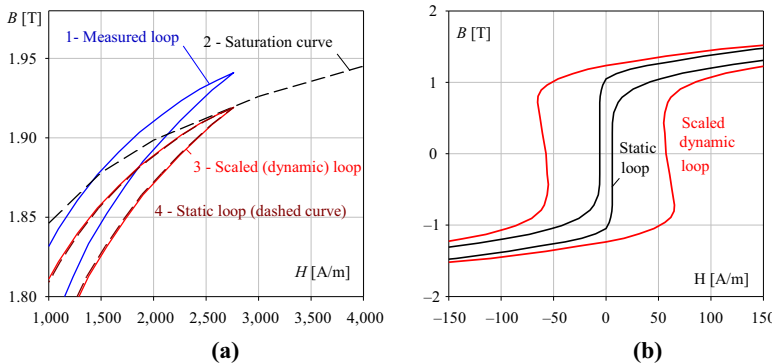
The $\psi-i$ curves deduced from voltage-current dependences measured on transformer terminals are often taken as characteristics of some core parts or even considered as saturation characteristics of the transformer as a whole, although this term is questionable in the case of a topological transformer model where $\psi-i$ characteristics seen from the LV and HV sides are quite different.

With this in mind, we can still begin the modeling with a simple numerical experiment in which the measured loop $\psi_{1A}-i_{1A}$ (Curve 1 in Figure 4) is used to restore $B-H$ loop of the core material. Following Fuchs and You (2002), there is nothing left but to omit air reluctances \mathfrak{R}_0 in Phases A and C of the model in Figure 2(a). This merges reluctances of the leg (\mathfrak{R}_A) and yoke (\mathfrak{R}_{AB}) into the equivalent reluctance \mathfrak{R}_{A-AB} of limb A. Using length l_A and cross-section S_A of the limb, the $\psi_{1A}-i_{1A}$ loop is recalculated into the loop $B_{meas}-H_{meas}$ using the well-known relationships, $B_{meas} = \Psi_{1A}/(N_1 S_A)$ and $H_{meas} = i_{1A} N_1 / l_A$. Here the length of limb A is the sum of lengths of the leg and yoke, $l_A = l_{leg} + l_{yoke}$.

The thus-obtained loop $B_{meas}-H_{meas}$ is shown in Figure 6(a) by the solid curve 1. It is remarkable that its tip lies markedly higher than the saturation curve 2 of steel M5 used in the accurate replication of the experimental $\psi_{1A}-i_{1A}$ loop in Zirka et al. (2022). Besides, there is uncertainty about the extension of loop 1 to large magnetic fields that can lead to mistakes in evaluating inrush currents and GIC effects.

The raised position of loop 1 in Figure 6(a) means that the upper (saturation) part of this curve represents not only the core steel but also linear inductances of the model. Indeed, if the core is far from saturation, small inductances L_0 and L_{01} in the model of Figure 2(d) are invisible compared to large inductances of the leg and yoke. However, when loop 1 approaches its tip, and the magnetic field increases to 2,700 A/m, the relative permeability of the core steel significantly drops, and inductances of the leg and yoke become comparable to L_0 and L_{01} .

To eliminate the influence of inductances L_0 and L_{01} at large magnetic fields and thus approach the $B-H$ loop of the core steel, different scalings of the measured loop 1 can be used. A simplest one is a vertical shrinking of the parent loop 1 using a scale factor k_s , whereby $B = k_s B_{meas}$. Here, the value of $k_s = 0.991$ was chosen so that the tip of the scaled



Source: Authors' own work

Figure 6.
(a) Measured and scaled loops of transformer T74; (b) dynamic and static loops

loop 3 in Figure 6(a) would lie on the saturation curve 2, which is a *static* catalog curve. To reduce the dynamic (50-Hz) loop 3 to the static loop $H_{\text{stat}}(B)$, the width of loop 3 is decreased proportionally to dB/dt , that is, proportionally to the measured voltage v_{A1} . For example, the ascending branch is formed as $k(dB/dt)H_{\text{meas}}$, where the multiplier k is chosen so that the coercive field of the loop is equal to 6–8 A/m, which is typical for GO steels. In case the static loop thus obtained exhibits negative slopes, corresponding segments are changed by vertical ones. After such correction, the static loop of the core steel of transformer T74 takes the shape shown in Figure 6(b).

When using the ATPDraw, the ascending branch of the static B – H loop is entered into the DHM hysteretic inductors (Høidalen *et al.*, 2021), which are reduced to the SHM-inductors by nullifying coefficient K_{loss} responsible for classical eddy current and excess losses. The choice of the user-defined material 0 allows one to use an arbitrary static loop defined in an external file. One should not be embarrassed by almost vertical static loop in Figure 6(b) and the slightly tilted dynamic loop in that figure. This inconsistency is then eliminated by using appropriate capacitance C .

The loops ψ_{1A} – i_{1A} calculated using the model in Figures 2(c) and (d) are shown by curves 2 and 4 in Figure 4, where lower parts of the larger (420 V) loops are also depicted in the inset. These loops are calculated for a capacitance $C = 0.18$ nF, providing the desired slope of the calculated loop in its middle part. At such a small C , inductances L_G should be omitted in the model. Resistances R_L of 2 k Ω provide the needed width of the calculated terminal loop in Figures 3(a) and 4. As the loops obtained are close to those calculated in Zirka *et al.* (2022), the no-load and inrush currents of transformer T74 are also close to the measured one.

3.3 The modeling of transformer T90

The core of a newer transformer, T90, was assembled from HGO laminations. Therefore, the saturation curve of the HGO steel 27ZDKH85 in Figure 5 was used in the model. In principle, the same technique as before was used for modeling transformer T90. It was found that different pairs of L_G and C provide the negative slope of terminal loop ψ_{1A} – i_{1A} measured in the saturation test. It was observed that decreasing C and a corresponding increase in L_G results in increasing the frequency of oscillations superimposed on the calculated loop. The loop in Figure 3(b) was found acceptable; it was calculated using $C = 1.2$ nF, $L_G = 3,000$ mH and $R_L = 4$ k Ω .

4. The modeling of no-load and inrush currents

The no-load currents of transformer T74 calculated with the model in Figure 2(c) are shown by solid lines in Figure 7(a). As specified in Subsection 3.2, no inductances L_G are required in the model to reproduce the saturation test results at $C = 0.18$ nF. Overall, the calculated currents A and C are close to the measured ones in Figure 7(b), which are asymmetric with respect to abscissa due to experimental uncertainties. The underestimation of current B in Figure 7(a) can be related to the fact that no information about behavior of leg B was obtained in the saturation test (Albert *et al.*, 2021). If the current B peaks have to be increased, inductance L_G of phase B can be introduced in the model. The corresponding increase in current B obtained with $L_G = 1,400$ mH is shown in Figure 7(a) by the dashed line. The calculated no-load loss (181 W) practically coincides with the nameplate loss (178 W).

The calculated inrush currents (solid curves in Figure 8) are in close agreement with currents (dashed curves) drawn by the unloaded transformer T74 from a public grid. The closest 315 kVA transformer of the grid and the feeding three-phase cable (200 m length)

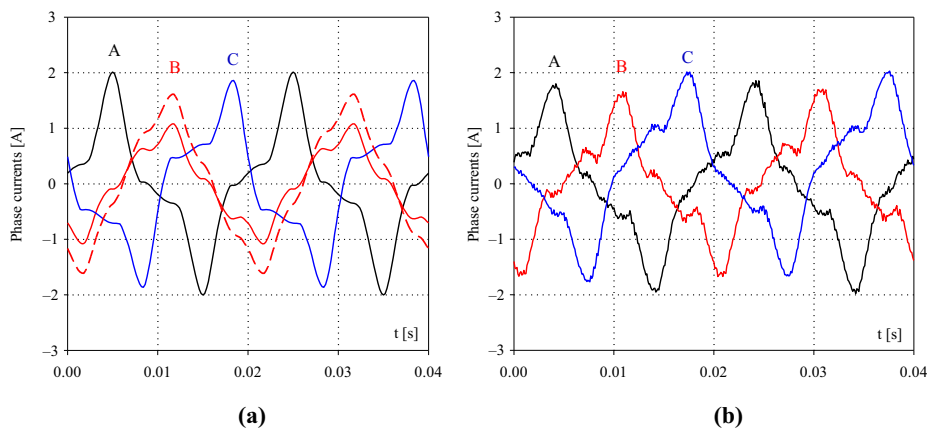


Figure 7.
(a) Calculated and (b)
measured no-load
currents

Source: Authors' own work

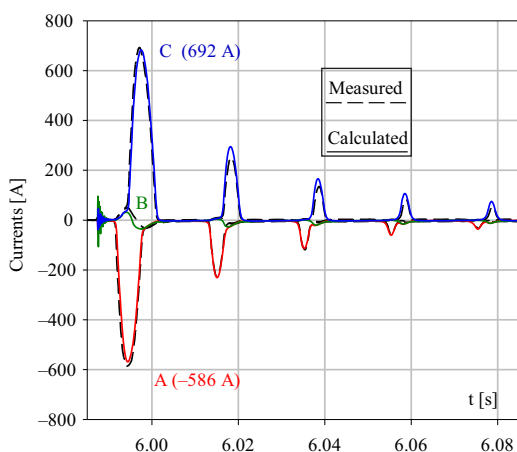


Figure 8.
Calculated and
measured inrush
currents

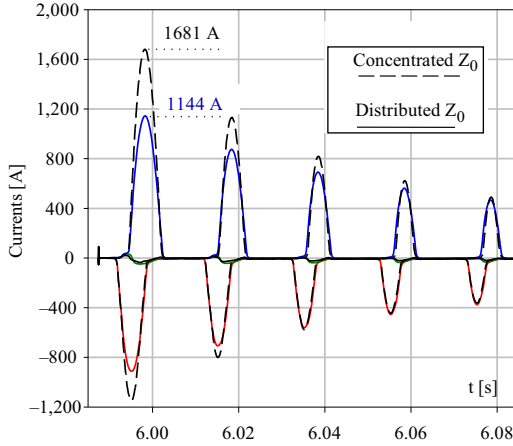
Source: Authors' own work

were represented in the model by a per phase inductance of 0.09 mH and by resistance of 0.137 Ω . Residual flux densities in legs A, B and C of the modeled transformer were estimated as $B_A(0) = -0.2$ T, $B_B(0) = -0.1$ T and $B_C(0) = +0.3$ T (Zirka *et al.*, 2022). These values were entered in the DHM-inductors of corresponding legs and yokes.

A smoothing influence of the grid can be seen when comparing the highest current peak (692 A) in Figure 8 with that (1,144 A in Figure 9) calculated for the same conditions but using an ideal, zero-impedance grid.

Another inaccuracy (it is illustrated by the increase of the current peak from 1,144 to 1,681 A in Figure 9) is introduced by concentrating the ZS impedance Z_0 of the transformer at its center leg, as made in a wide range of transformer models. To show the fallacy of that approach and justify the distribution of Z_0 between three legs, the standard ZS test was

Figure 9.
Inrush currents
calculated with ideal
grid



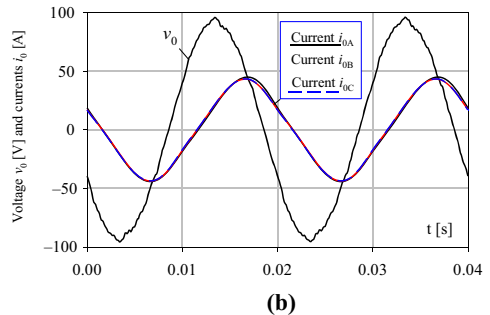
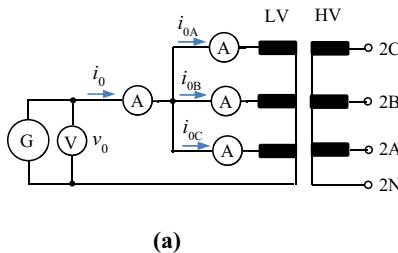
Source: Authors' own work

supplemented for the first time with measurements of currents i_{0A} , i_{0B} and i_{0C} in all phase windings, [Figure 10\(a\)](#). The practical coincidence of these currents in [Figure 10\(b\)](#) validates the necessity of the even distribution of Z_0 accepted in the model proposed.

5. Conclusion

The presented modeling of two three-phase three-legged 50 kVA transformers is based on terminal voltages and currents measured in a special purpose saturation test. The terminal ψ - i loops are recalculated in effective B - H loops of the gapped core material, taking into account a typical saturation curve of grain-oriented electrical steel. The B - H loops obtained are then used in individual hysteretic inductors of the legs and yokes used in the transformer topological model. The need for the equal distribution of the ZS elements between all three legs was proven by almost equal ZS currents measured in each phase winding. The presented measurement-based approach was successfully tested in steady state and transient regimes of the modeled transformers whose cores are assembled from CGO and HGO electrical steels. The use of the model proposed for predicting transformer behavior under DC grid voltages will be demonstrated in subsequent papers.

Figure 10.
(a) Enhanced zero-
sequence test used,
and (b) currents
measured during the
ZS test on
transformer T74



Source: Authors' own work

References

- Albert, D., Maletic, D. and Renner, H. (2021), "Measurement based transformer modelling approach", Proc. ETG Congr., pp. 1-6. [Online], available at: <https://ieeexplore.ieee.org/document/9469662>
- Biró, O., Buchgraber, G., Leber, G. and Preis, K. (2008), "Prediction of magnetizing current waveforms in a three-phase power transformer under dc bias", *IEEE Transactions on Magnetics*, Vol. 44 No. 6, pp. 1554-1557, doi: [10.1109/TMAG.2007.916041](https://doi.org/10.1109/TMAG.2007.916041).
- Chiesa, N., Mork, B.A. and Høidalen, H.K. (2010), "Transformer model for inrush current calculations: simulations, measurements and sensitivity analysis", *IEEE Transactions on Power Delivery*, Vol. 25 No. 4, pp. 2599-2608, doi: [10.1109/TPWRD.2010.2045518](https://doi.org/10.1109/TPWRD.2010.2045518).
- Chisepo, H.K., Borrill, L.D. and Gaunt, C.T. (2018), "Measurements show need for transformer core joint details in finite element modelling of GIC and DC effects", *COMPEL – The International Journal for Computation and Mathematics in Electrical and Electronic Engineering*, Vol. 37 No. 3, pp. 1011-1028, doi: [10.1108/COMPEL-11-2016-0511](https://doi.org/10.1108/COMPEL-11-2016-0511).
- Fuchs, E.F. and You, Y. (2002), "Measurement of λ -i characteristics of asymmetric three-phase transformers and their applications", *IEEE Transactions on Power Delivery*, Vol. 17 No. 4, pp. 983-990, doi: [10.1109/TPWRD.2002.803702](https://doi.org/10.1109/TPWRD.2002.803702).
- Hernández, I., Cañedo, J.M., Olivares-Galván, J.C. and Georgilakis, P.S. (2011), "Electromagnetic analysis and comparison of conventional-wound cores and octagonal-wound cores of distribution transformers", *Materials Science Forum*, Vol. 670, pp. 477-486, doi: [10.4028/www.scientific.net/MSF.670.477](https://doi.org/10.4028/www.scientific.net/MSF.670.477).
- Høidalen, H.K., Prikler, L. and Peñaloza, F. (2021), *ATPDRAW Version 7.0 for Windows. Users' Manual*, NTNU, Trondheim, Norway.
- Martínez, J.A., Walling, R., Mork, B.A., Martín-Arnedo, J. and Durbak, D. (2005), "Parameter determination for modeling system transients – Part III: transformers", *IEEE Transactions on Power Delivery*, Vol. 20 No. 3, pp. 2051-2062, doi: [10.1109/TPWRD.2005.848752](https://doi.org/10.1109/TPWRD.2005.848752).
- Moses, P.S., Masoum, M.A.S. and Toliyat, H.A. (2010), "Dynamic modeling of three-phase asymmetric power transformers with magnetic hysteresis: no-load and inrush conditions", *IEEE Transactions on Energy Conversion*, Vol. 25 No. 4, pp. 1040-1047, doi: [10.1109/TEC.2010.2065231](https://doi.org/10.1109/TEC.2010.2065231).
- Pedra, J., Sainz, L., Córcoles, F., Lopez, R. and Salichs, M.A. (2004), "PSPICE computer model of a nonlinear three-phase three-legged transformer", *IEEE Transactions on Power Delivery*, Vol. 19 No. 1, pp. 200-207, doi: [10.1109/TPWRD.2003.820224](https://doi.org/10.1109/TPWRD.2003.820224).
- Zirka, S.E., Albert, D., Moroz, Y.I. and Renner, H. (2022), "Further improvements in topological transformer model covering core saturation", *IEEE Access*, Vol. 10, pp. 64018-64027, doi: [10.1109/ACCESS.2022.3183279](https://doi.org/10.1109/ACCESS.2022.3183279).
- Zirka, S.E., Moroz, Y.I., Chiesa, N., Harrison, R.G. and Høidalen, H.K. (2015a), "Implementation of inverse hysteresis model into EMTP – part i: static model", *IEEE Transactions on Power Delivery*, Vol. 30 No. 5, pp. 2233-2241, doi: [10.1109/TPWRD.2015.2416199](https://doi.org/10.1109/TPWRD.2015.2416199).
- Zirka, S.E., Moroz, Y.I., Chiesa, N., Harrison, R.G. and Høidalen, H.K. (2015b), "Implementation of inverse hysteresis model into EMTP – Part ii: dynamic model", *IEEE Transactions on Power Delivery*, Vol. 30 No. 5, pp. 2233-2241, doi: [10.1109/TPWRD.2015.2416199](https://doi.org/10.1109/TPWRD.2015.2416199).
- Zirka, S.E., Moroz, Y.I., Elovaara, J., Lahtinen, M., Walling, R.A., Høidalen, H., Bonmann, D., Arturi, C. M. and Chiesa, N. (2018), "Simplified models of three-phase, five-limb transformer for studying GIC effects", *Int. J. Electric Power and Energy Systems*, Vol. 103, pp. 168-175, doi: [10.1016/j.ijepes.2018.05.035](https://doi.org/10.1016/j.ijepes.2018.05.035).
- Zirka, S.E., Moroz, Y.I., Harrison, R.G. and Chiesa, N. (2014), "Inverse hysteresis models for transient simulation", *IEEE Transactions on Power Delivery*, Vol. 29 No. 2, pp. 552-559, doi: [10.1109/TPWRD.2013.2274530](https://doi.org/10.1109/TPWRD.2013.2274530).

About the authors



Sergey E. Zirka received the PhD and DSc degrees in Electrical Engineering from the Institute of Electrodynamics, Kiev, Ukraine, in 1977 and 1992, respectively. Since 1972, he has been with the Dnepropetrovsk (now Dnipro) National University, Ukraine, where he has been a Professor since 1992. His research interests include the modeling of Magnetization Processes in electrical steels, hysteresis models, forming and transforming high-energy pulses and transients in transformers of different types. <https://orcid.org/0000-0001-7607-1436>



Dennis Albert received the MSc degree in Electrical Engineering from RWTH Aachen University, Germany and the PhD degree in Electrical Engineering from Graz University of Technology in 2022. Since 2022, he works as an Application Engineer at OMCIRON Electronics GmbH in Austria. His field of research includes power transformer modeling and diagnostics. <https://orcid.org/0000-0001-8916-851X> Dennis Albert is the corresponding author and can be contacted at: dennis.albert@tugraz.at



Yuriy I. Moroz received the PhD degree in Theoretical Electrical Engineering from the Institute of Modeling Problems in Energetics, the Ukrainian Academy of Sciences, Kiev, Ukraine, in 1991. Currently, he is an Associate Professor with the Department of Physics and Technology at Dnipro National University, Ukraine. His research interests include the modeling of magnetization processes in electrical steels and transients in transformers of different types. <https://orcid.org/0000-0001-7696-1324>



Lukas Daniel Domenig is a PhD student at the Institute of Fundamentals and Theory in Electrical Engineering at Graz University of Technology, Austria. His main research interests are Electromagnetic Network Models and Finite Element Methods, including hysteresis operators.



Robert Schürhuber studied Electrical Engineering and Technical Mathematics at the Vienna University of Technology, where he also received his PhD in 2002 in the field of Theoretical Electrical Engineering. He then worked in industry for 15 years in various areas of power engineering, including the control and regulation of thermal plants, the planning and design of electrical plants and system aspects of large-scale hydropower. In 2017, he was appointed to the Graz University of Technology, where he has since headed the Institute of Electrical Systems and Grids. His main research interests are in the field of short circuit calculations, stability of converter connected units and mathematical modeling of power systems.